AIP | Applied Physics Letters

Solid phase epitaxial growth of high mobility La:BaSnO3 thin films co-doped with interstitial hydrogen

Christian A. Niedermeier, Sneha Rhode, Sarah Fearn, Keisuke Ide, Michelle A. Moram, Hidenori Hiramatsu, Hideo Hosono, and Toshio Kamiya

Citation: Applied Physics Letters **108**, 172101 (2016); doi: 10.1063/1.4948355
View online: http://dx.doi.org/10.1063/1.4948355
View Table of Contents: http://scitation.aip.org/content/aip/journal/apl/108/17?ver=pdfcov
Published by the AIP Publishing

Solid phase epitaxial growth of high mobility La:$BaSnO_3$ thin films co-doped with interstitial hydrogen

Christian A. Niedermeier,[1,2,a] Sneha Rhode,[1] Sarah Fearn,[1] Keisuke Ide,[2] Michelle A. Moram,[1] Hidenori Hiramatsu,[2,3] Hideo Hosono,[2,3] and Toshio Kamiya[2,3]
[1]*Department of Materials, Imperial College London, Exhibition Road, London SW7 2AZ, United Kingdom*
[2]*Materials and Structures Laboratory, Tokyo Institute of Technology, Mailbox R3-4, 4259 Nagatsuta, Midori-ku, Yokohama 226-8503, Japan*
[3]*Materials Research Center for Element Strategy, Tokyo Institute of Technology, 4259 Nagatsuta, Midori-ku, Yokohama 226-8503, Japan*

(Received 16 March 2016; accepted 15 April 2016; published online 28 April 2016)

This work presents the solid phase epitaxial growth of high mobility La:$BaSnO_3$ thin films on $SrTiO_3$ single crystal substrates by crystallization through thermal annealing of nanocrystalline thin films prepared by pulsed laser deposition at room temperature. The La:$BaSnO_3$ thin films show high epitaxial quality and Hall mobilities up to $26 \pm 1\,cm^2/Vs$. Secondary ion mass spectroscopy is used to determine the La concentration profile in the La:$BaSnO_3$ thin films, and a 9%–16% La doping activation efficiency is obtained. An investigation of H doping to $BaSnO_3$ thin films is presented employing H plasma treatment at room temperature. Carrier concentrations in previously insulating $BaSnO_3$ thin films were increased to $3 \times 10^{19}\,cm^{-3}$ and in La:$BaSnO_3$ thin films from $6 \times 10^{19}\,cm^{-3}$ to $1.5 \times 10^{20}\,cm^{-3}$, supporting a theoretical prediction that interstitial H serves as an excellent n-type dopant. An analysis of the free electron absorption by infrared spectroscopy yields a small (H,La):$BaSnO_3$ electron effective mass of $0.27 \pm 0.05\ m_0$ and an optical mobility of $26 \pm 7\,cm^2/Vs$. As compared to La:$BaSnO_3$ single crystals, the smaller electron mobility in epitaxial thin films grown on $SrTiO_3$ substrates is ascribed to threading dislocations as observed in high resolution transmission electron micrographs. *Published by AIP Publishing.* [http://dx.doi.org/10.1063/1.4948355]

Transparent conducting oxides (TCOs) combine low electrical resistivity with high optical transparency and find important applications in optoelectronic devices as transparent contacts for solar cells, electron injection layers for light emitting diodes, and high mobility electron transport layers for flat panel displays. Indium tin oxide (ITO) is the most widely employed TCO due to its excellent electronic conductivity above 1×10^4 Scm and high optical transparency,[1] but its relative scarcity and the high demand for indium from competing applications make it increasingly expensive to use.

The extraordinary high carrier mobility of $320\,cm^2/Vs$ recently reported for $BaSnO_3$ single crystals at a carrier concentration of $8 \times 10^{19}\,cm^{-3}$ (Ref. 2) has triggered research efforts to improve and understand the electronic transport in $BaSnO_3$ epitaxial thin films.[3–8] Besides its potential for commercial application as a transparent conductor composed of abundant elements, La:$BaSnO_3$ epitaxial thin films may find applications as a high-mobility channel layer in multifunctional perovskite-based electronic devices and field-effect transistors.[9–11] Room temperature Hall mobilities as high as $70\,cm^2/Vs$ have been reported for vapour phase-grown epitaxial thin films at a doping level of $4 \times 10^{20}\,cm^{-3}$ prepared by pulsed laser ablation of 4–7 at. % La:$BaSnO_3$ targets.[2] Epitaxial thin films prepared by molecular beam epitaxy show Hall mobilities of $81\,cm^2/Vs$ at a doping level of $1.65 \times 10^{20}\,cm^{-3}$ for 4 at. % La:$BaSnO_3$ (Ref. 12) and $150\,cm^2/Vs$ at a doping level of $7 \times 10^{19}\,cm^{-3}$.[8] Despite La substitutional doping well beyond the 3 at. % equilibrium solubility limit in $BaSnO_3$,[13–15] the actual La composition in the thin films has rarely been investigated.

This work presents the solid phase epitaxial growth of high mobility La:$BaSnO_3$ thin films by crystallization through thermal annealing of nanocrystalline thin films prepared by pulsed laser deposition (PLD) at room temperature. Since growth of high-quality epitaxial La:$BaSnO_3$ thin films requires high growth temperatures of 750–900 °C,[3,4,8,12] solid phase epitaxy is advantageous for epitaxial growth because the high temperature process may be separated from the vacuum deposition and easily performed in a conventional furnace. Moreover, thin films of single crystal-like structure can be obtained applying solid phase epitaxy, as demonstrated for $In_2O_3(ZnO)_m$ ($m = $ integer)[16] and LaCuOS[17,18] epitaxial thin films. The actual La solubility after epitaxial crystallization and the La doping activation efficiency is determined by secondary ion mass spectroscopy (SIMS). This work further presents H doping to $BaSnO_3$ thin films as implemented by H plasma treatment at room temperature. First principles calculations of interstitial H in $BaSnO_3$ indicate a low formation energy comparable to that of substitutional La on the Ba site,[19] but no experimental studies have been reported. After H indiffusion, the previously insulating undoped $BaSnO_3$ thin films become highly conductive with Hall mobilities of $15 \pm 1\,cm^2/Vs$, suggesting interstitial H as the second most effective n-type dopant after La reported up to date. The co-doped (H,La):$BaSnO_3$ thin films show enhanced free carrier absorption, and the optical mobility and the electron effective mass are assessed from Fourier transform infrared (FT-IR) spectra.

Polycrystalline $BaSnO_3$ and 7 at. % La:$BaSnO_3$ targets for PLD were prepared from high purity $BaCO_3$, SnO_2, and

[a]Author to whom correspondence should be addressed. Electronic mail: c.niedermeier13@imperial.ac.uk

La_2O_3 powders by solid state ceramic processing. Rietveld refinement of the X-ray diffraction (XRD) pattern of the 7 at. % La:$BaSnO_3$ target showed that it is composed of two phases, 96.9 wt. % $La_xBa_{1-x}SnO_3$ (space group Pm-3m, ICSD 186899) and 3.1 wt. % $La_2Sn_2O_7$ (space group Fd-3m, ICSD 153813). $SrTiO_3$ (100) single crystal substrates were etched in NH_4F-buffered HF solution (pH 4.5) for 3 min and annealed at 1050 °C for 1 h in air to obtain a TiO_2-terminated step-and-terrace surface.[20,21] Nanocrystalline 100 nm thick (La:)$BaSnO_3$ thin films were deposited at room temperature and 7 Pa O_2 pressure using a 248 nm KrF laser with a fluence of 2 J/cm^2 at a pulse frequency of 10 Hz.

The as-deposited La:$BaSnO_3$ thin film was covered with the polished side of a yttria stabilized zirconia single crystal substrate and annealed at 1100 °C for 1 h in air to induce the epitaxial crystallization. The crystal structure was investigated by high resolution X-ray diffraction (HR-XRD) employing a Rigaku SmartLab diffractometer with a monochromatic Cu $K_{\alpha 1}$ (1.5406 Å) X-ray source and parallel beam optics. Interstitial H doping of (La:)$BaSnO_3$ thin films was implemented by H indiffusion during plasma treatment at room temperature in 10 Pa H_2 atmosphere applying a radio frequency power of 50 W for 1 min. The electron transparent cross-sectional TEM specimen was prepared by grinding, polishing, and dimpling until the specimen thickness was below 10 μm, followed by Ar ion milling using a PIPS Ion miller (Gatan USA). Conventional and high resolution transmission electron microscopy (HR-TEM) was performed using a JEOL 2100 microscope equipped with a field emission gun operating at 200 keV.

An IONTOF time-of-flight SIMS was used to analyse the H and La concentration profiles in the (H,La):$BaSnO_3$ thin films. 1 keV Cs^+ and a 25 keV Bi^+ primary ion beams were used for sputtering and analysis in an area of 300 μm^2 and 100 μm^2, respectively. Alternating current Hall measurements were performed with a ResiTest 8300 system (Toyo Co.) using the four-terminal method and van der Pauw geometry. Temperature-dependent electrical transport properties were measured in the range from 300 K to 80 K in He atmosphere. The optical transmission and reflectivity of the (H,La):$BaSnO_3$ thin films were measured with a Hitachi U-4100 UV-VIS-NIR and a Bruker Optics VERTEX70v FT-IR spectrophotometer.

The HR-XRD pattern of the La:$BaSnO_3$ thin film on $SrTiO_3$ substrate after solid phase crystallization at 1100 °C indicates the (100)-oriented epitaxial growth (Fig. 1(a)). The low degree of mosaicity of La:$BaSnO_3$ thin films is indicated by the narrow, 0.07° full width at half maximum (FWHM) rocking curve of the La:$BaSnO_3$ 200 diffraction (Fig. 1(b)). The in-plane and out-of-plane lattice parameters of 4.107 Å and 4.108 Å of the La:$BaSnO_3$ thin film are close to the $La_xBa_{1-x}SnO_3$ unstrained lattice parameter of 4.120 Å obtained by Rietveld refinement of the XRD pattern of the 7 at. % La:$BaSnO_3$ target (Fig. 1(c)). It is concluded that the thin films are almost completely relaxed due to the 5.5% lattice mismatch with the $SrTiO_3$ substrate and the high-temperature crystallization process.

The (H,La):$BaSnO_3$ thin film microstructure is investigated by cross-sectional bright-field (BF) TEM acquired under two-beam conditions near the ⟨100⟩ zone axis (Fig. 2(a)). An

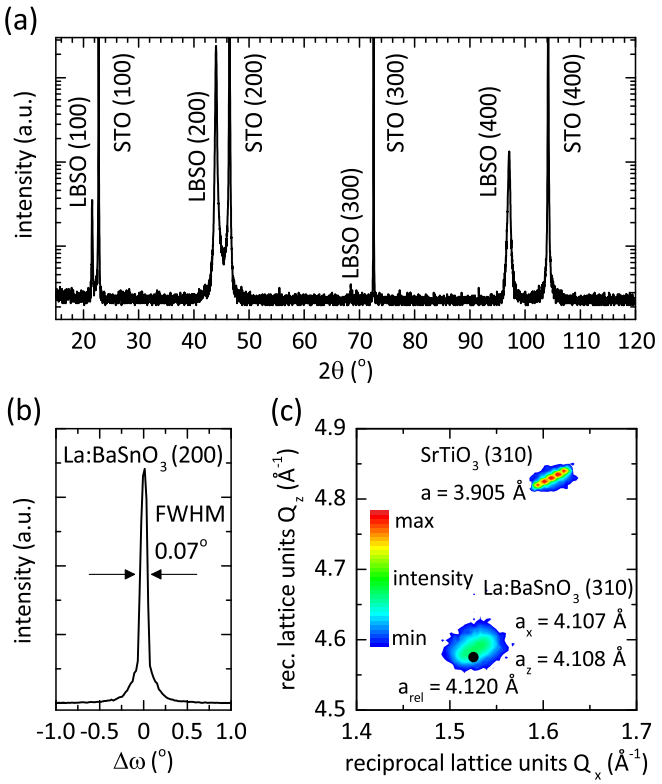

FIG. 1. (a) HR-XRD pattern of La:$BaSnO_3$ thin film after solid phase epitaxial growth at 1100 °C showing the (100)-oriented growth on the $SrTiO_3$ substrate. (b) Narrow, 0.07° FWHM rocking curve of the La:$BaSnO_3$ 200 diffraction indicating the high crystalline quality. (c) Reciprocal space map of the 310 diffraction given by an equidistant iso-intensity contour map on a logarithmic scale. The epitaxial La:$BaSnO_3$ thin film is fully relaxed, and the narrow diffraction spot relative to the $SrTiO_3$ single crystal substrate diffraction indicates the low degree of mosaicity.

array of equidistant misfit dislocations is observed at the interface between the (H,La):$BaSnO_3$ thin film and the $SrTiO_3$ substrate, and threading dislocations which proceed through the bulk of the film are indicated with thin arrows. Cross-sectional HR-TEM micrographs acquired along the ⟨100⟩ zone axis show 7.7 nm equidistant misfit dislocations at the La:$BaSnO_3$/$SrTiO_3$ interface marked with bold arrows (Figs. 2(b) and 2(c)). Applying the measured in-plane La:$BaSnO_3$ and $SrTiO_3$

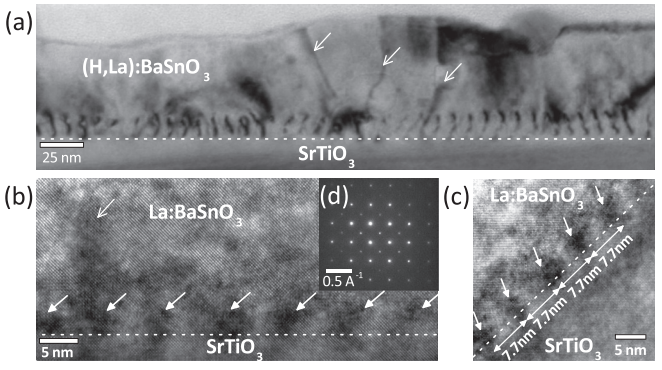

FIG. 2. (a) BF cross-sectional TEM micrograph of the (H,La):$BaSnO_3$ thin film showing misfit dislocations along the (H,La):$BaSnO_3$/$SrTiO_3$ interface and threading dislocations (thin arrows) proceeding through the bulk of the film. (b) and (c) Cross-sectional HR-TEM micrographs showing the array of misfit dislocations (bold arrows) along the La:$BaSnO_3$/$SrTiO_3$ interface with an equidistant 7.7 nm spacing. (d) Corresponding selected area diffraction pattern of the La:$BaSnO_3$ thin film.

lattice parameters obtained in the 310 reciprocal space map analysis, a theoretical misfit dislocation spacing of $a_{LBSO} \times a_{STO}/(a_{LBSO} - a_{STO}) = 7.9$ nm is obtained. The selected-area electron diffraction pattern obtained for the La:$BaSnO_3$ thin film confirms the La:$BaSnO_3$ (100)||$SrTiO_3$ (100) epitaxial relationship (Fig. 2(d)).

The SIMS depth-profile of a 80-nm (H,La):$BaSnO_3$ thin film after solid phase crystallization shows that the $LaOH^-/SnO_2^-$ intensity ratio is constant over the entire depth profile indicating that La is uniformly distributed (Fig. 3(a)). Employing experimentally derived sensitivity factors with reference to the intensities obtained for the 7 at. % La:$BaSnO_3$ target, a La concentration of 7.4 ± 1.5 at. % is obtained. It follows that the La composition in the La:$BaSnO_3$ thin films is maintained during both room temperature PLD and solid phase crystallization at 1100 °C. As compared to the H^- profile of a La:$BaSnO_3$ thin film without intentional H doping, the H concentration in the co-doped (H,La):$BaSnO_3$ thin film is remarkably enhanced over the entire depth of the film confirming H indiffusion during the plasma treatment.

The La solubility in $La_xBa_{1-x}SnO_3$ determined in this work is about 4 at. %, as obtained from the weight fractions of 96.9% La:$BaSnO_3$ and 3.1% $La_2Sn_2O_7$ after Rietveld refinement of the XRD pattern of the two-phasic 7 at. % La:$BaSnO_3$ target. Epitaxial stabilization of the La:$BaSnO_3$ thin films may promote La doping beyond the solubility limit without formation of a secondary phase. However, since the obtained La:$BaSnO_3$ thin film lattice parameters are similar to that of bulk 4 at. % La:$BaSnO_3$, excess La may have segregated at domain boundaries or likewise formed a secondary $La_2Sn_2O_7$ phase. These phases would not be identified by HR-XRD analysis due to the random orientation and small crystallite size.

The La:$BaSnO_3$ thin films show Hall mobilities of up to 26 ± 1 cm^2/Vs (Fig. 3(b)), which is the highest among the films prepared by PLD with carrier concentrations as low as 6×10^{19} cm^{-3}. Assuming that every La atom may contribute one free electron, the measured Hall carrier concentration of 9.0×10^{19} cm^{-3} for the La:$BaSnO_3$ thin film yields a La dopant activation efficiency of 9%–16%, depending on the actual La concentration in the La:$BaSnO_3$ grains of 4–7 at. %. The low La doping activation efficiency may be attributed to threading dislocations which may create deep electronic levels and trap carriers. Thus a high La doping concentration is required for screening of the defects before free carriers may be introduced that contribute to a high mobility.[4,7]

Undoped $BaSnO_3$ thin films are insulating, but after H plasma treatment they become highly conductive with Hall mobilities of 15 ± 1 cm^2/Vs, which is similar to that of the La:$BaSnO_3$ thin films but obtained at a doping level of only 3.3×10^{19} cm^{-3}. H co-doping of La:$BaSnO_3$ thin films raises the doping level from about 8×10^{19} cm^{-3} to 1.6×10^{20} cm^{-3} and is found to be reversible as confirmed by high vacuum annealing.[21] Since for most semiconductors the H^+/H^- charge transition level lies virtually constant at about 4.5 eV below the vacuum level, interstitial H may form a shallow donor if its level lies well inside the conduction band.[22–24] In analogy to ZnO and SnO_2, $BaSnO_3$ demonstrates a sufficiently high electron affinity to be doped by interstitial H.[21] The large dispersion of the $BaSnO_3$ conduction band arising from the Sn 5s orbital as well as the ideal 180° Sn–O–Sn bond angle in the network of corner sharing $[SnO_6]^{2-}$ octahedra in the cubic perovskite structure are seen as the key factors for the high mobility.[25] Since interstitial H does not perturb the electron conduction path through the $[SnO_6]^{2-}$ octahedra network, similar mobilities are achieved by both H- and La-doping. For example, Sb-doping on the Sn-site in Sb:$BaSnO_3$ is less beneficial as it results in inferior electronic transport and Hall mobilities as compared to La:$BaSnO_3$ (Refs. 7 and 26) and H:$BaSnO_3$. Thus, interstitial H is suggested as the second most effective n-type dopant for $BaSnO_3$ after La reported up to date.

The La:$BaSnO_3$ thin film shows enhanced IR absorption after co-doping with H (Fig. 4(a)). The pronounced optical absorption in the region of 2000–6000 cm^{-1} observed in FT-IR spectra is attributed to the free carrier absorption in the (H,La):$BaSnO_3$ thin film by comparison with the bare $SrTiO_3$ single crystal substrate (Fig. 4(b)). The dielectric function $\epsilon(\omega)$ of the (H,La):$BaSnO_3$ thin film in the IR spectral region is calculated by fitting theoretical transmission

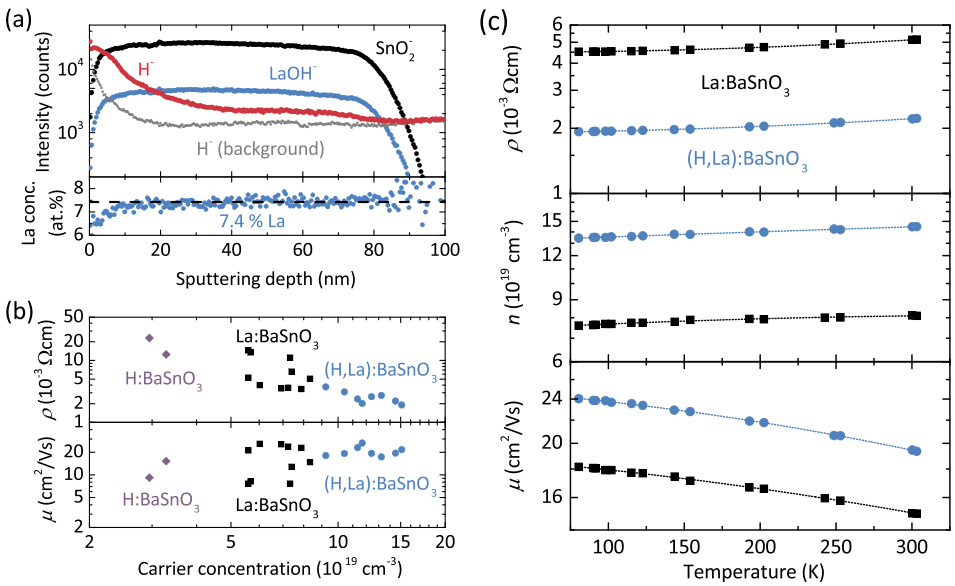

FIG. 3. (a) SIMS depth profile of co-doped (H,La):$BaSnO_3$ thin film after solid phase crystallization at 1100 °C and subsequent H plasma treatment. The La doping concentration is evaluated by employing experimentally determined sensitivity factors. (b) Electrical resistivity and Hall mobility for several H- and/or La-doped $BaSnO_3$ thin films as a function of carrier concentration. Co-doped (H,La):$BaSnO_3$ thin films exhibit the highest carrier concentrations of about 1.6×10^{20} cm^{-3}. (c) The temperature-independent carrier concentration of both La:$BaSnO_3$ and co-doped (H,La):$BaSnO_3$ thin film indicates degenerated semiconductor (metal-like) electronic transport behaviour.

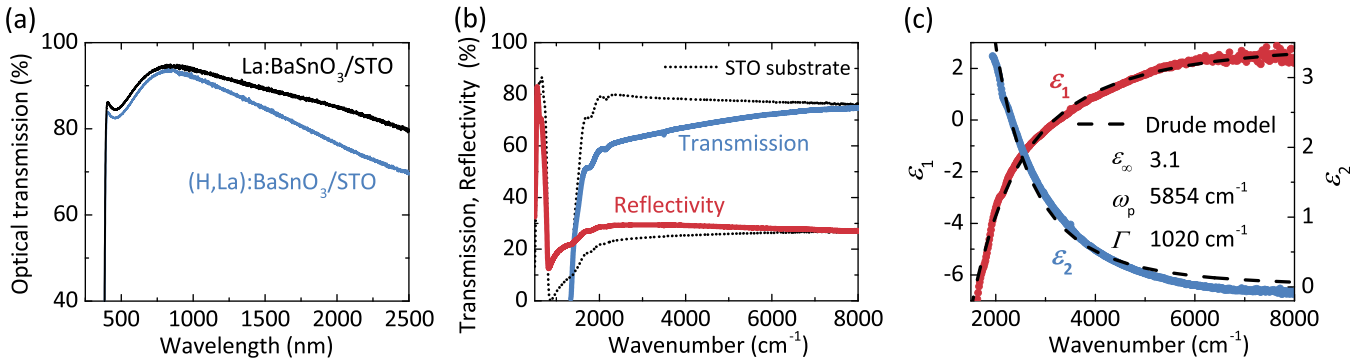

FIG. 4. (a) Optical transparency of a La:$BaSnO_3$ thin films on $SrTiO_3$ substrate before and after H plasma treatment. The higher free carrier density in the H-doped La:$BaSnO_3$ is indicated by the enhanced IR absorption. (b) The IR optical transmission and reflectivity of the (La,H):$BaSnO_3$ thin film and of the bare $SrTiO_3$ substrate. (c) The dielectric function of (H,La):$BaSnO_3$ obtained by IR transmission and reflectivity spectra is well fitted by the Drude free-electron model describing the free carrier absorption.

and reflectivity spectra to the measured ones at each data point (point-by-point analysis) with accounting for the dielectric function of the $SrTiO_3$ substrate (Fig. 4(c)). It is described by the Drude free-electron model

$$\epsilon(\omega) = \epsilon_\infty - \frac{\omega_p^2}{\omega^2 - i\Gamma\omega},$$

where ω is the wavenumber, ϵ_∞ is the high frequency dielectric constant, ω_p is the plasma frequency, and Γ is the diffusion frequency. The parameters used in the analytical model allow for calculation of the optical mobility $\mu = \frac{\epsilon_0 \omega_p^2}{ne\Gamma}$ and electron effective mass $m^* = \frac{ne^2}{\omega_p^2 \epsilon_0}$ of the (H,La):$BaSnO_3$ thin films. Here, ϵ_0 is the vacuum permittivity, n is the measured Hall carrier concentration, and e is the electron charge. Since the optical mobility and the electron effective mass vary with the square of plasma frequency, the error in determination of these parameters for a single specimen is large. Thus, an average optical mobility of $26 \pm 7\,cm^2/Vs$ and electron effective mass 0.27 ± 0.05 m_0 of (H,La):$BaSnO_3$ thin films is determined from a series of specimens.

The electrical mobility μ in a semiconductor is determined from the equilibrium electron drift velocity obtained after the acceleration force due to the applied potential and the friction force due to scattering effects are in balance. It is described by

$$\mu = \frac{e\tau}{m^*},$$

where m^* is the electron effective mass and τ is the momentum relaxation time denoting the average time of momentum loss by scattering. As compared to other high mobility TCOs such as ZnO, In_2O_3, and SnO_2, the (H,La):$BaSnO_3$ electron effective mass of 0.27 ± 0.05 m_0 is similarly small, indicating a large contribution to the high mobility (Table I).

The optical mobility of $26 \pm 7\,cm^2/Vs$ obtained for (H,La):$BaSnO_3$ thin films from IR optical spectra is about equal to the electron mobility obtained by Hall measurements, suggesting that scattering of electrons at grain boundaries is insignificant. The negative slope of the mobility-temperature relation indicating the non-thermally activated electron transport behaviour (Fig. 3(c)) is typical for highly degenerate semiconductors, in which trapped charges at grain boundaries may be screened by the high density free electron gas, thereby reducing the effective barrier height for intergranular transport.[30] It is suggested that dislocations act as electron acceptors and the charged defects may reduce the optical mobility by long-range Coulombic interaction with carriers. Charged dislocation scattering is strongly screened due to the high carrier density and explains why for La:$BaSnO_3$ the Hall mobility generally increases with carrier concentration.

In conclusion, the La:$BaSnO_3$ solid phase epitaxial growth presents an effective method to obtain high mobility thin films of high crystal quality using the room temperature-deposited nanocrystalline phase as precursor. The La dopant activation of about 9%–16% is attributed to dislocations in epitaxial La:$BaSnO_3$ thin films which act as carrier traps. Interstitial H doping presents the second most effective n-type doping method after substitutional La doping reported up to date. As compared to La:$BaSnO_3$ thin films, H:$BaSnO_3$ thin films show a similarly high mobility of $15 \pm 1\,cm^2/Vs$, but at a doping level of only $3.3 \times 10^{19}\,cm^{-3}$.

The small electron effective mass of 0.27 ± 0.05 m_0 contributes to the high $29 \pm 1\,cm^2/Vs$ mobility observed for epitaxial co-doped (H,La):$BaSnO_3$ thin films. Both the

TABLE I. Comparison of the electron effective mass of high mobility TCOs ZnO, (H,La):$BaSnO_3$, SnO_2, and In_2O_3.

TCO	Electron effective mass (m_0)	Method	Reference
ZnO	0.23	Cyclotron resonance	27
(H,La):$BaSnO_3$	0.27 ± 0.05	FT-IR spectroscopy	This work
SnO_2	0.28	Cyclotron resonance	28
In_2O_3	0.34	First-principles calculation	29

TEM observation of the high density of misfit dislocations which are the source for threading dislocations and the nearly temperature-independent electron mobility suggest that charged dislocation scattering is the main cause for the reduced electron mobility in epitaxial (H,La):$BaSnO_3$ thin films.

C. A. Niedermeier acknowledges the support through an international research fellowship provided by the Japan Society for the Promotion of Science (JSPS). The work at Tokyo Institute of Technology was supported by the Ministry of Education, Culture, Sports, Science, and Technology (MEXT) Element Strategy Initiative to Form Core Research Center. H. Hiramatsu was also supported by the Japan Society for the Promotion of Science (JSPS) through a Grant-in-Aid for Scientific Research on Innovative Areas "Nano Informatics" Grant No. 25106007, and Support for Tokyotech Advanced Research (STAR).

[1]H. Ohta, M. Orita, M. Hirano, H. Tanji, H. Kawazoe, and H. Hosono, "Highly electrically conductive indium-tin-oxide thin films epitaxially grown on yttria-stabilized zirconia (100) by pulsed-laser deposition," Appl. Phys. Lett. **76**, 2740 (2000).
[2]H. J. Kim, U. Kim, H. M. Kim, T. H. Kim, H. S. Mun, B.-G. Jeon, K. T. Hong, W.-J. Lee, C. Ju, K. H. Kim, and K. Char, "High mobility in a stable transparent perovskite oxide," Appl. Phys. Express **5**, 061102 (2012).
[3]H. J. Kim, U. Kim, T. H. Kim, J. Kim, H. M. Kim, B.-G. Jeon, W.-J. Lee, H. S. Mun, K. T. Hong, J. Yu, K. Char, and K. H. Kim, "Physical properties of transparent perovskite oxides (Ba,La)SnO_3 with high electrical mobility at room temperature," Phys. Rev. B **86**, 165205 (2012).
[4]H. Mun, U. Kim, H. Min Kim, C. Park, T. Hoon Kim, H. Joon Kim, K. Hoon Kim, and K. Char, "Large effects of dislocations on high mobility of epitaxial perovskite $Ba_{0.96}La_{0.04}SnO_3$ films," Appl. Phys. Lett. **102**, 252105 (2013).
[5]S. Sallis, D. O. Scanlon, S. C. Chae, N. F. Quackenbush, D. A. Fischer, J. C. Woicik, J.-H. Guo, S. W. Cheong, and L. F. J. Piper, "La-doped $BaSnO_3$—degenerate perovskite transparent conducting oxide: Evidence from synchrotron x-ray spectroscopy," Appl. Phys. Lett. **103**, 042105 (2013).
[6]P. V. Wadekar, J. Alaria, M. O'Sullivan, N. L. O. Flack, T. D. Manning, L. J. Phillips, K. Durose, O. Lozano, S. Lucas, J. B. Claridge, and M. J. Rosseinsky, "Improved electrical mobility in highly epitaxial La:$BaSnO_3$ films on $SmScO_3$(110) substrates," Appl. Phys. Lett. **105**, 052104 (2014).
[7]U. Kim, C. Park, T. Ha, R. Kim, H. S. Mun, H. M. Kim, H. J. Kim, T. H. Kim, N. Kim, J. Yu, K. H. Kim, J. H. Kim, and K. Char, "Dopant-site-dependent scattering by dislocations in epitaxial films of perovskite semiconductor $BaSnO_3$," APL Mater. **2**, 056107 (2014).
[8]S. Raghavan, T. Schumann, H. Kim, J. Y. Zhang, T. A. Cain, and S. Stemmer, "High-mobility $BaSnO_3$ grown by oxide molecular beam epitaxy," APL Mater. **4**, 016106 (2016).
[9]C. Park, U. Kim, C. J. Ju, J. S. Park, Y. M. Kim, and K. Char, "High mobility field effect transistor based on $BaSnO_3$ with Al_2O_3 gate oxide," Appl. Phys. Lett. **105**, 203503 (2014).
[10]U. Kim, C. Park, T. Ha, Y. M. Kim, N. Kim, C. Ju, J. Park, J. Yu, J. H. Kim, and K. Char, "All-perovskite transparent high mobility field effect using epitaxial $BaSnO_3$ and $LaInO_3$," APL Mater. **3**, 036101 (2015).
[11]Y. M. Kim, C. Park, U. Kim, C. Ju, and K. Char, "High-mobility $BaSnO_3$ thin-film transistor with HfO_2 gate insulator," Appl. Phys. Express **9**, 011201 (2016).
[12]Z. Lebens-Higgins, D. O. Scanlon, H. Paik, S. Sallis, Y. Nie, M. Uchida, N. F. Quackenbush, M. J. Wahila, G. E. Sterbinsky, D. A. Arena, J. C. Woicik, D. G. Schlom, and L. F. J. Piper, "Direct observation of electrostatically driven band gap renormalization in a degenerate perovskite transparent conducting oxide," Phys. Rev. Lett. **116**, 027602 (2016).
[13]M. Trari, J.-P. Doumerc, P. Dordor, M. Pouchard, G. Behr, and G. Krabbes, "Preparation and characterization of lanthanum doped $BaSnO_3$," J. Phys. Chem. Solids **55**, 1239 (1994).
[14]M. Yasukawa, T. Kono, K. Ueda, H. Yanagi, and H. Hosono, "High-temperature thermoelectric properties of La-doped $BaSnO_3$ ceramics," Mater. Sci. Eng.: B **173**, 29 (2010).
[15]X. Luo, Y. S. Oh, A. Sirenko, P. Gao, T. A. Tyson, K. Char, and S.-W. Cheong, "High carrier mobility in transparent $Ba_{1-x}La_xSnO_3$ crystals with a wide band gap," Appl. Phys. Lett. **100**, 172112 (2012).
[16]K. Nomura, H. Ohta, K. Ueda, M. Orita, M. Hirano, and H. Hosono, "Novel film growth technique of single crystalline $In_2O_3(ZnO)_m$ (m = integer) homologous compound," Thin Solid Films **411**, 147 (2002).
[17]H. Hiramatsu, K. Ueda, H. Ohta, M. Orita, M. Hirano, and H. Hosono, "Heteroepitaxial growth of a wide-gap p-type semiconductor, LaCuOS," Appl. Phys. Lett. **81**, 598 (2002).
[18]H. Hiramatsu, H. Ohta, T. Suzuki, C. Honjo, Y. Ikuhara, K. Ueda, T. Kamiya, M. Hirano, and H. Hosono, "Mechanism for heteroepitaxial growth of transparent P-type semiconductor: LaCuOS by reactive solid-phase epitaxy," Cryst. Growth Des. **4**, 301 (2004).
[19]D. O. Scanlon, "Defect engineering of $BaSnO_3$ for high-performance transparent conducting oxide applications," Phys. Rev. B **87**, 161201 (2013).
[20]M. Kawasaki, K. Takahashi, T. Maeda, R. Tsuchiya, M. Shinohara, O. Ishiyama, T. Yonezawa, M. Yoshimoto, and H. Koinuma, "Atomic control of the $SrTiO_3$ crystal surface," Science **266**, 1540 (1994).
[21]See supplementary material at http://dx.doi.org/10.1063/1.4948355 for the surface topography of $SrTiO_3$ substrates and La:$BaSnO_3$ thin films, thermal desorption spectra and the position of the H^+/H^- charge transition level in $BaSnO_3$.
[22]C. G. Van de Walle, "Hydrogen as a cause of doping in zinc oxide," Phys. Rev. Lett. **85**, 1012 (2000).
[23]C. Kilic and A. Zunger, "n-type doping of oxides by hydrogen," Appl. Phys. Lett. **81**, 73 (2002).
[24]C. G. Van de Walle and J. Neugebauer, "Universal alignment of hydrogen levels in semiconductors, insulators and solutions," Nature **423**, 626 (2003).
[25]H. Mizoguchi, H. W. Eng, and P. M. Woodward, "Probing the electronic structures of ternary perovskite and pyrochlore oxides containing Sn^{4+} or Sb^{5+}," Inorg. Chem. **43**, 1667 (2004).
[26]H. J. Kim, J. Kim, T. H. Kim, W.-J. Lee, B.-G. Jeon, J.-Y. Park, W. S. Choi, D. W. Jeong, S. H. Lee, J. Yu, T. W. Noh, and K. H. Kim, "Indications of strong neutral impurity scattering in Ba(Sn,Sb)O_3 single crystals," Phys. Rev. B **88**, 125204 (2013).
[27]M. Oshikiri, Y. Imanaka, F. Aryasetiawan, and G. Kido, "Comparison of the electron effective mass of the n-type ZnO in the wurtzite structure measured by cyclotron resonance and calculated from first principle theory," Phys. B: Condens. Matter **298**, 472 (2001).
[28]K. J. Button, C. G. Fonstad, and W. Dreybrodt, "Determination of the electron masses in stannic oxide by submillimeter cyclotron resonance," Phys. Rev. B **4**, 4539 (1971).
[29]Y. Mi, H. Odaka, and S. Iwata, "Electronic structures and optical properties of ZnO, SnO_2 and In_2O_3," Jpn. J. Appl. Phys. **38**, 3453 (1999).
[30]Z. M. Jarzebski, "Preparation and physical properties of transparent conducting oxide films," Phys. Status Solidi (A) **71**, 13 (1982).